DESIGN AND OPERATION OF THE PRINCETON-PENNSYLVANIA PROTON SYNCHROTRON

H. L. Allen, G. K. O'Neill, P. J. Reardon, J. Riedel, L. Seidlitz, F. C. Shoemaker, E. P. Tomlinson, M. G. White

(Presented by M. G. WHITE)

1. OBJECTIVE

The Princeton-Pennsylvania Accelerator was started in 1956 with the following objectives in mind: 1) to provide an average current of 3 GeV proton 10 to 100 times higher than was available at that time; 2) to provide shielding adequate for an eventual average current of 1 μA or 3 kW of beam; 3) to provide flexibility in shielding design to accommodate future external proton beams.

2. BASIC DESIGN

In previous International Accelerator Conferences we have described the Princeton-Pennsylvania Accelerator (PPA) in some detail [1, 2]; so this paper will serve merely to bring the design up-to-date and to report on actual performance of various components. The PPA is a weak focussing ($n = 0.60 \div 0.58$) synchrotron with good «n» region at injection of 6.1 × 16.5 cm. In order to obtain high average currents, the pulse rate was made 19 cps, or nearly 100 times the normal pulse rate for machines of this size. From the outset it was recognized that the combination of small aperture and fast pulsing would impose very severe tolerances on magnet design, vacuum chamber construction, injection system and, especially, the radio-frequency acceleration system. Also the expected high average beam power was expected to raise severe radiation damage problems. These anticipated difficulties were all encountered, and to a large extent, solved.

The high pulse rate of 19 cps practically demanded that the magnetic gap be drastically reduced in volume from that used in other 3 GeV synchrotrons; otherwise the magnet power problem would have become excessively large. Therefore, in so far as space charge limitations are involved, we cannot expect to contain as much charge per pulse as, say, the Cosmotron by about the ratio of «good n» volumes. Even so, our pulse rate advantage should give us a factor of ten more on average current. On the other hand, if space charge is not the limiting factor, as would be the case were we to inject at 25 MeV, or when polarized protons or heavy ions are accelerated, then we should realize our full pulse rate advantage of 100. Courant [3] has pointed out that, unlike other accelerators, the Princeton-Pennsylvania Accelerator, because of its 8-fold symmetry, should have no difficulty with depolarization of protons during acceleration.

3. MAGNET DESIGN

Fig. 1 shows the magnet as completed. Details of the magnetic measurements that were made and the required mechanical tolerances are given in the paper by P. J. Reardon, L. Seidlitz, and F. C. Shoemaker [4] presented at this conference. In view of the very small aperture of 6.1 × 16.5 cm, it is clear that every precaution was necessary to achieve a good field shape over the magnetic field range of 260 ÷ 14,000 Gs. Our decision to rely on «crenelated» pole tips rather than the usual high power corrective windings normally used at high fields, served, however, to increase the need for extreme care in mechanical design and construction of the magnet, the pole tips, and the clamping.

Mechanically the magnet is very tight and free from excessive vibration, though it is necessary carefully to avoid resonance in all auxiliary equipment fastened to the magnet. Fig. 2 shows how we employ pneumatic pressure tubes to clamp the pole tips, their spacers, and the magnet yoke into a very tight unit. After an initial period of pneumatic hose failures a fully satisfactory design was eventually devised. Coil clamping was carried out in a very careful manner, so that essentially no coil motion is observable.

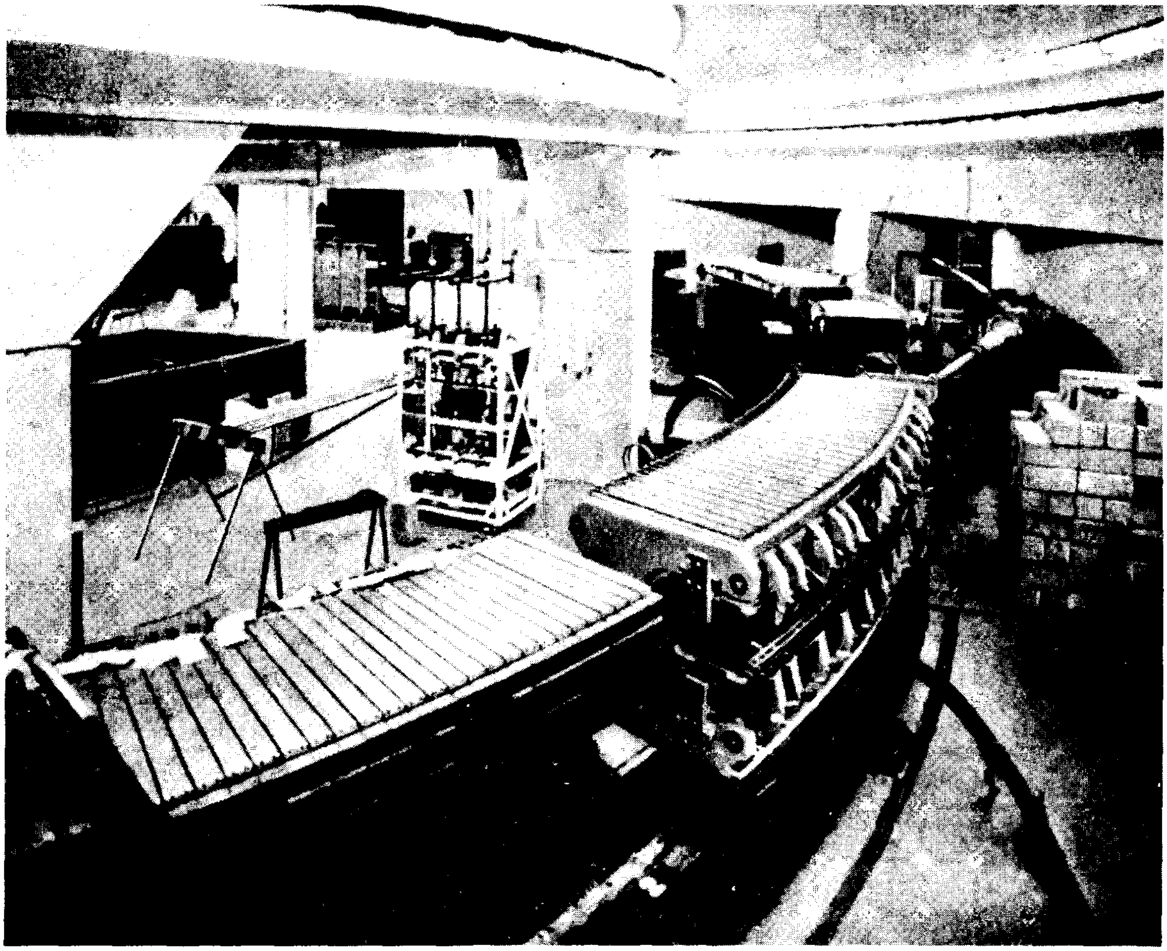

Fig. 1. Photograph of magnet.

4.. MAGNET POWER SUPPLY

The 19 cps pulse rate clearly required that the magnet be resonated with a capacitor bank. Furthermore, it was very early established that a dc bias would be required to minimize the ac losses in the magnet and to simplify the radio-frequency acceleration problem. The circuit chosen is shown in Fig. 2 which differs from that given at CERN in 1956 by the very important addition of 16 equalizer windings to the transformer-reactor. Not only to these windings provide a very simple way to introduce the alternating current, but they also shift the various unwanted oscillation modes away from the desired fundamental mode. A further dividend is that they equalize the distribution of voltage across each series capacitor, in spite of possible fault conditions and capacity unbalances, so that lower voltage rated capacitors may be safely used.

Power is provided by a 3000 kW synchronous motor connected through an eddy current clutch to a single power shaft which drives the dc and ac machines. By varying clutch drag, we can run the ac alternator resonant with the magnet system. The Q of the magnet circuit is about 70, which requires that the ac alternator be locked to the magnet with a phase error precision of 10^{-3} rad or to a frequency precision of 10^{-3}%. This has proven to be entirely feasible. Overall stability is excellent and no difficulty is experienced in maintaining the minimum magnetic field at 270 $\pm$ 1/2 Gs. The precision actually achieved may be better appreciated by noting that since the minimum magnetic field is the difference of two large numbers, the ac and the dc components, it is necessary to achieve separate ac and dc stabilities to better than 1/14,000. Fluctuations in B_{min} affect not only the initial injection process, but also have an even more pronounced effect, through variations in dB/dt, on the RF frequency and amplitude functions. A program of cleaning up these small fluctuations and interactions is now under way in the belief that much of our pulse to pulse instability in beam current is due to $\dot{B}$ fluctuations.

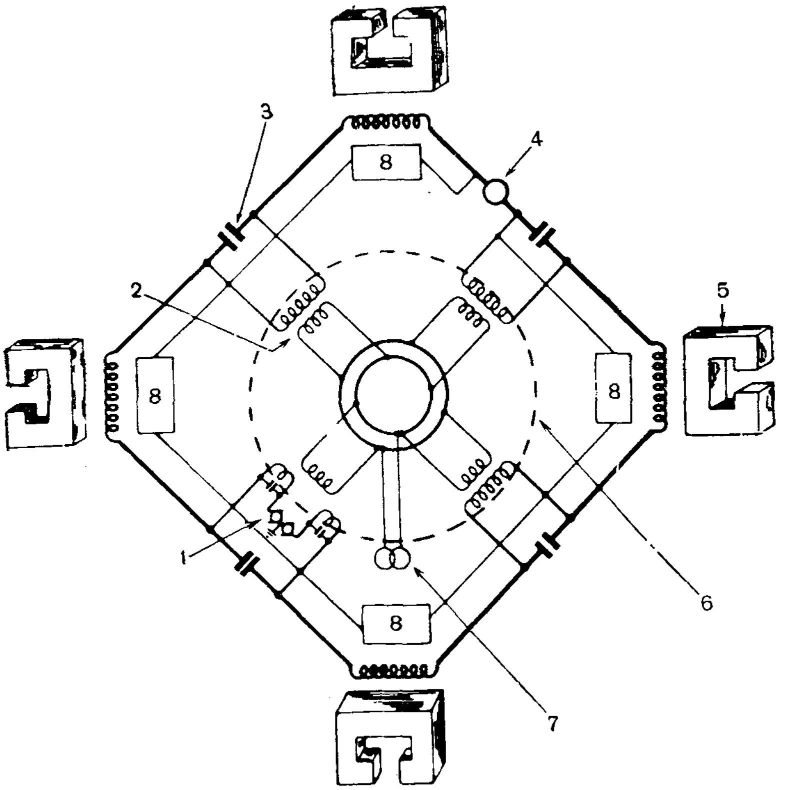

Fig. 2. Magnet power circuit with distributed capacitor bank and equalized reactor-transformer (drawn for magnet with only 4 sections): *1* — dc generators; *2* — primary equalizer; *3* — resonating capacitors; *4* — magnet current monitors; *5* — synchrotron magnet; *6* — reactor transformer eddy current shield; *7* — ac generator; *8* — B_{min} trimmer.

A prominent feature of the magnet resonant system is the large air-core transformer reactor shown in Fig. 3. It consists of 96 flat coils shunting the 16 series capacitors and 64 interleaved paralleled primary windings. The entire stack is carefully clamped against vibration and oil immersed for insulation and cooling. Though initially we encountered severe vibration problems which delayed us many months, the manufacturer has now entirely corrected them.

5. VACUUM CHAMBER

In order to conserve vertical aperture, the vacuum chamber, Fig. 4, was constructed of laminated metal ribs, firmly clamped to the front wall of stainless steel, and made vacuum tight by a thin skin of epoxy and fibre glass cloth. The ribs are a special alloy of copper-nickel (70/30) with permeability of $\mu - 1 = 0.002$. Full scale prototype measurements demonstrated no observable effect on «n». The front stainless steel wall, also serving double duty as a pole tip spacer, is in a region of high magnetic field and had to be water cooled in order to carry away eddy current induced heat. Even so, the temperature of the chamber ribs rises to 50° C after several hours of operation. This temperature rise, though not excessive, causes the epoxy to become more porous to water vapor, thereby raising the chamber pressure from 10^{-6} to 10^{-5} Torr. The problem was attacked by two approaches: 1) liquid nitrogen cooled pipes in the vacuum chamber; 2) stainless steel liner strips, 1/2 mil thick and 4 cm wide, inside the vacuum chamber. Using both these techniques reduces the operating pressure at running temperature to 5×10^{-7} Torr. More recently we have rebuilt one chamber using a 5 mil glass sheet in place of one layer of fibre glass. The porosity to water vapor and helium was reduced to almost zero. We believe that the use of glass sheets will eventually allow us to eliminate entirely the liquid nitrogen and also the need for the stainless steel liner. The use of thin sheets of glass in the epoxy coating may also reduce our radiation damage worries. Studies are underway to test this belief. Essentially all gaskets are soft aluminum which, once we learned the proper technique, have pro-

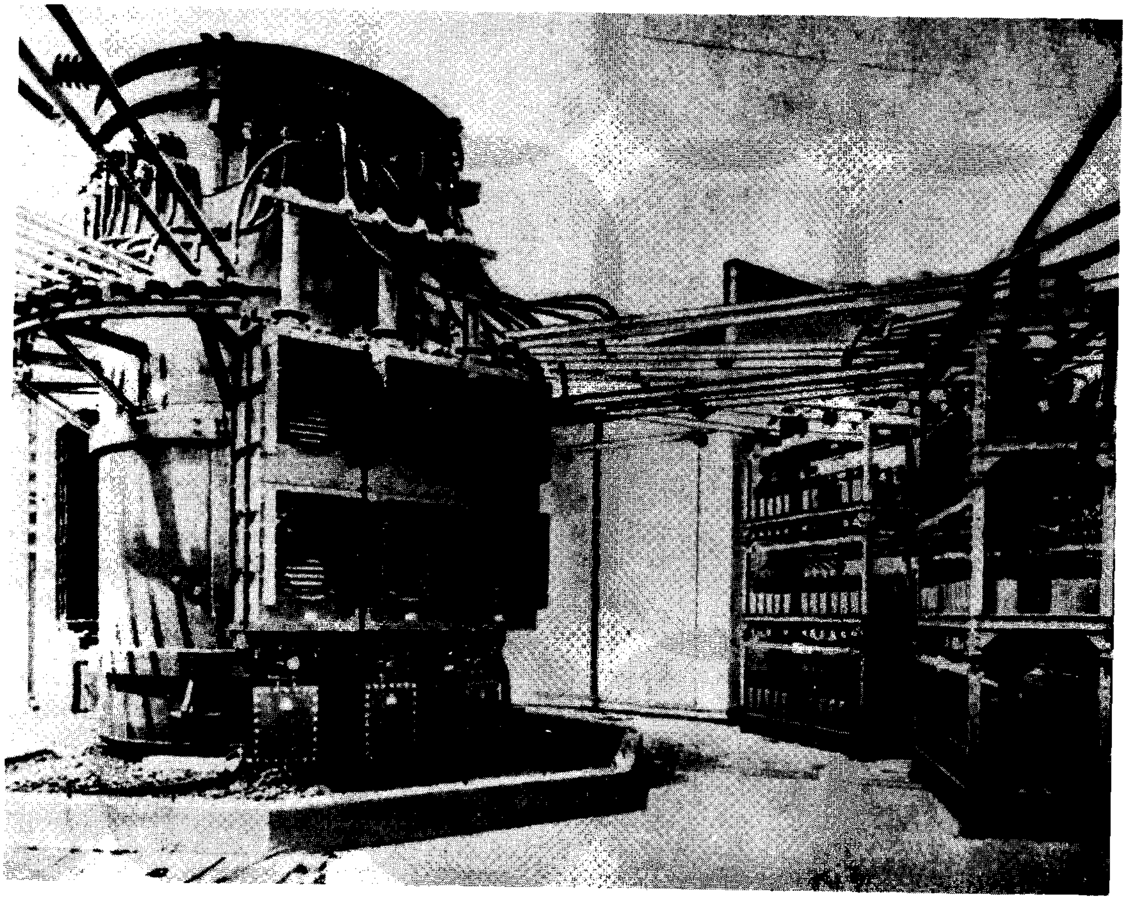

Fig. 3. Air-core transformer reactor.

ven to be extremely reliable. Evacuation takes place at 24 oil diffusion pump stations placed around the ring. A new pumping fluid Convolex-10, has been entirely trouble free, due in large part to its resistance to damage through overheating or exposure to air when hot. No liquid nitrogen cooled pump baffles are necessary.

6. INJECTION

The present injection technique calls for injecton with zero betatron oscillations on the instantaneous equilibrium orbit and at a $dB/dt = 44.3$ kGs/s which causes successive turns to shrink by 1.4 cm, thus missing the inflector plate. A 3 MeV Van de Graaff accelerator with capacitative liner, which can be raised to 35 kV in 30 μs, delivers a well focussed beam to the synchrotron through a series of electrostatic quadrupole lenses and deflector plates, see Fig. 5. Energy regulation to the desired ± 500 V has turned out to be a difficult problem, one on which we are still working. Ripple voltages as high as 10 kV at frequencies ranging from 6 cps were present in the machine as supplied by the manufacturer, but have been reduced to a little less than ± 1 kV by redesign. Rough, slow voltage control to ± 1500 V is achieved by running a 10 μA dc beam through the inflector, which bends the beam through 24°, and then sensing the energy error by a pair of pick-up plates on either side of the deflector exit. Actual voltage control is achieved by varying the corona current to the high voltage terminal. When the pulsed beam is bent by the synchrotron magnet into a circular path which is almost on the equilibrium orbit passing through the inflector, the beam strikes a pick-up plate thus initiating the various programmed voltages for the capacitative liner, the deflector, and the inflector. Fig. 6 shows the injection of 9 turns

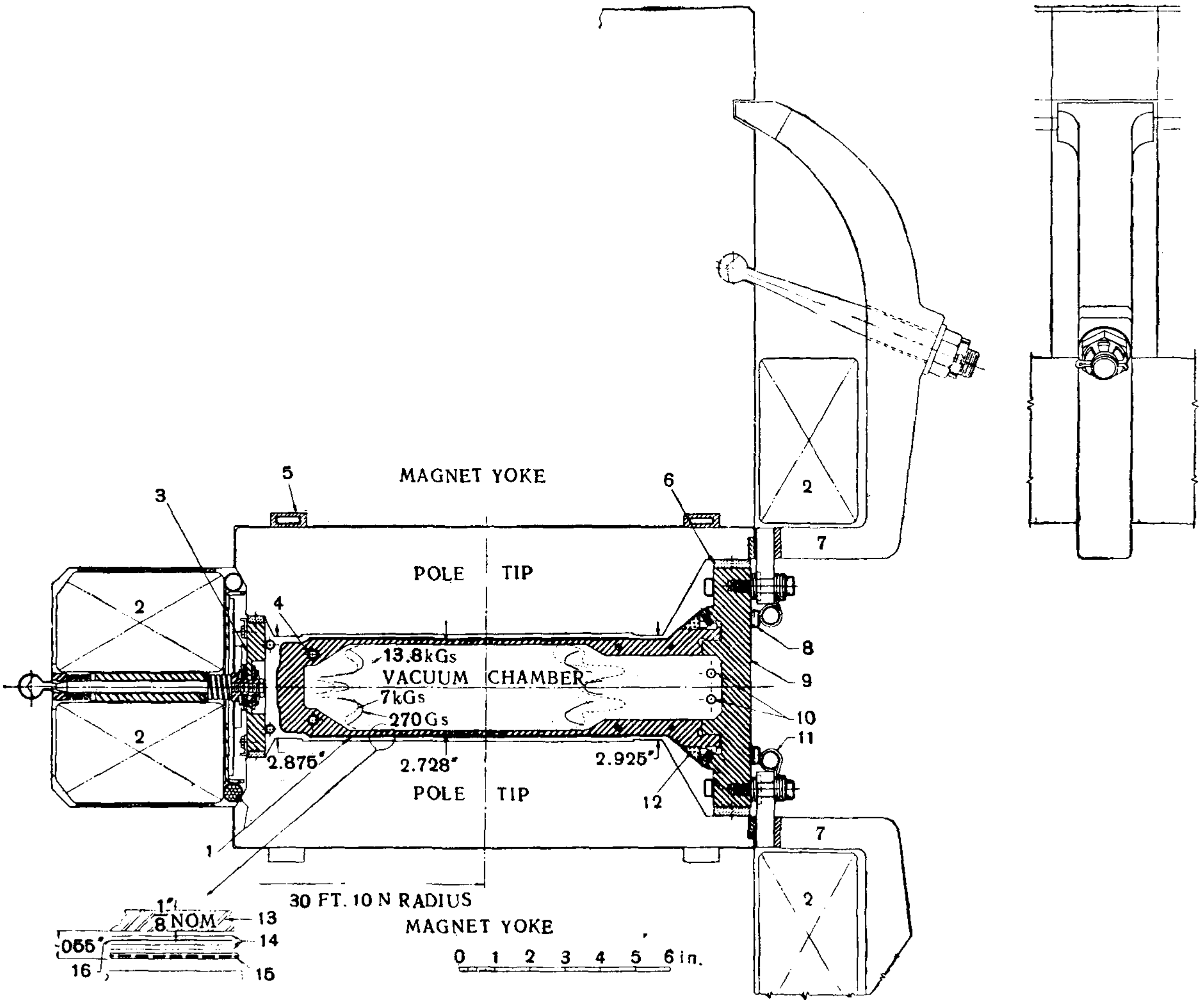

Fig. 4. Cross section of vacuum chamber and magnet pole tips. (Semi-aperture loss due to atmospheric load at center ~ 1/32"):

1 — correction coil windings and return; *2* — magnet coil; *3* — rear pole tip spacer; *4* — stainless steel tie rods; *5* — pneumatic clamping tube; *6* — ceramic spacer; *7* — pole tip clamp; *8* — water cooling; *9* — stainless steel chamber wall and front spacer; *10* — liquid nitrogen cold «fingers»; *11* — correction coil return; *12* — ceramic wedge; *13* — chamber wall copper-nickel alloy; *14* — glass cloth, glass sheet and epoxy; *15* — correction coil and glue line, 0.013" + 0.005" glue; *16* — glass micro sheet (vapor barrier).

before the beam strikes the back wall. Thus far we have obtained about 1.5 mA of protons out of the Van de Graaff of which about 20% enters the synchrotron producing a measured charge of about 2×10^{10} protons in the vacuum chamber before RF turn-on. We expect to be able to inject about 2×10^{11} protons per pulse with the present injector system after it is «cleaned» up, while an improved ion source, «on the drawing board», should increase this injected charge to 10^{12} protons. RF capture efficiency we will discuss later in this article.

Using a 3/4 μs duration injected pulse, we have studied the magnetic field perturbations and after trimming up the injection field in each semi-octant by ± 0.3%, we have succeeded in obtaining a closed orbit which departs from the ideal orbit by only ± 1 cm (Fig. 6). Vertical oscillations are very small since the beam stays in the median plane to ± 0.5 cm. In Fig. 6 the top trace shows «sum» signals induced in 2 pick-up stations, spaced 180° around the magnet ring, as the charge pulse makes 9 trips around the ring. The bottom trace is the so-called difference signal whose

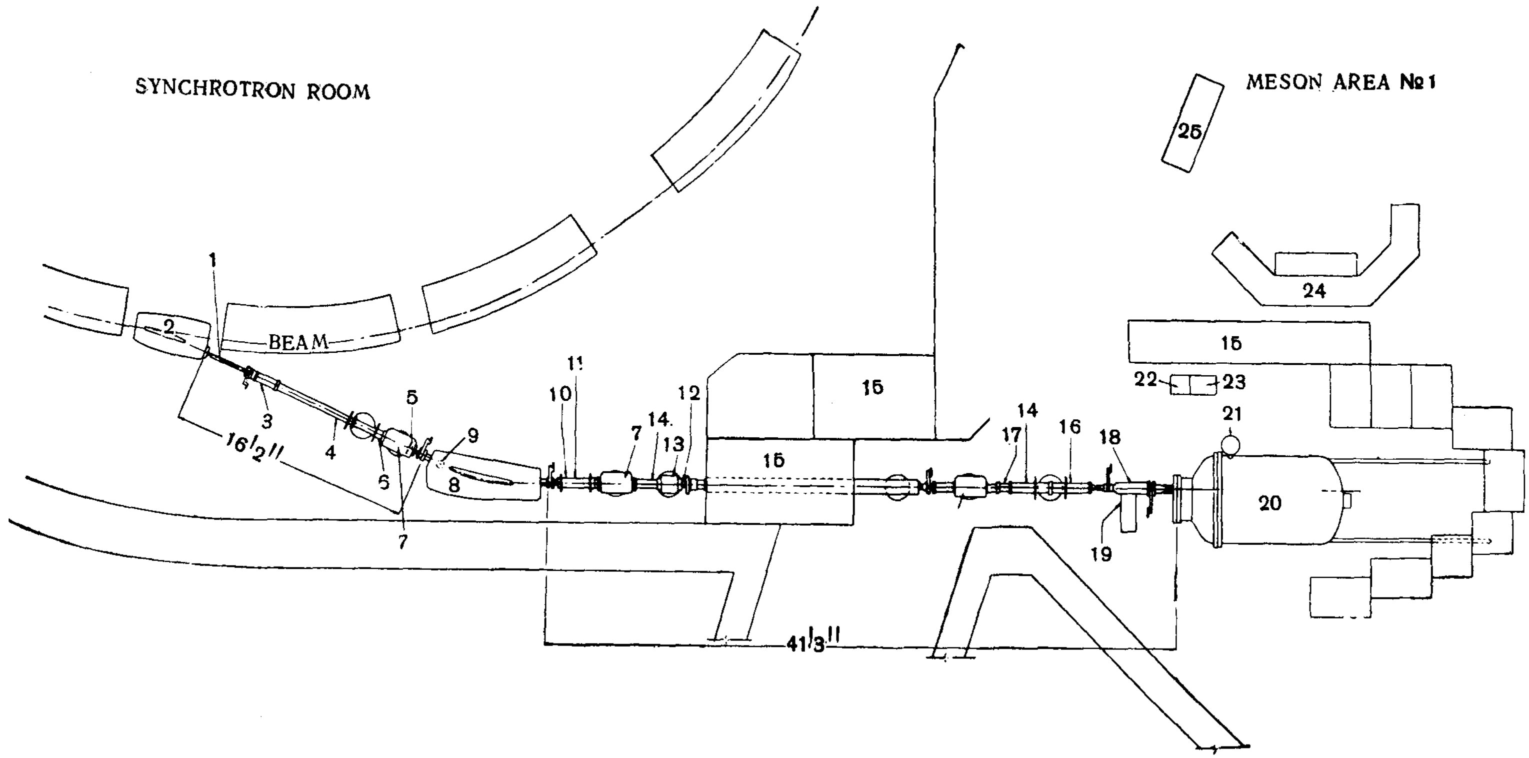

Fig. 5. Injection system-plan view:

1 — 2″ beam deflecting coils; *2* — inflector; *3* — steering plates; *4* — 4″ beam deflecting coils; *5* — Van de Graaff slow loop energy control slits; *6* — vacuum pump station No. 5; *7* — beam viewing box; *8* — deflector; *9* — vacuum pump station No. 4; *10* — 6″ beam deflecting coils; *11* — electrostatic quadrupole pair lens; *12* — vacuum pump station No. 3; *13* — beam monitor box; *14* — electrostatic steering plates; *15* — shielding blocks; *16* — beam chopper; *17* — vacuum pump station No. 2; *18* — 6″ pump; *19* — vacuum pump station No. I; *20* — acceleration tube, 3 MeV Van de Graaff generator, 4 : 1 mixture of N_2 and CO_2 at 300 psig; *21* — liner pulser transformer (35 kV peak pulse for 30 μs); *22* — belt charge control; *23* — belt charge power supply; *24* — injection control panel; *25* — inflector-deflector power supply (25—75 kV dc).

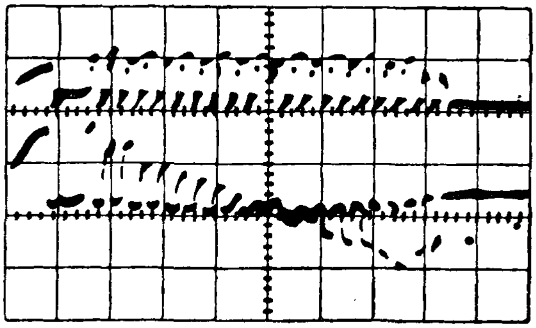

Fig. 6. Sum and difference signals from a $^3/_4$ μs chopped injected beam.

amplitude is proportional to the radial position of the charge pulse with respect to the middle of the vacuum chamber. A positive pulse indicates that the beam is at a radius larger than that of the middle of the vacuum chamber.

7. RADIO-FREQUENCY SYSTEM

Without doubt, our most complex, most difficult design problem has been the radio-frequency system. Though we can successfully accelerate to 3 GeV about 5% of the injected protons, we are still improving the reliability and the precision of the system. Luckily, transistors were invented just in time to make practicable the large number of servo loops which are required to achieve the required stability. In another paper presented to this conference [5], we go

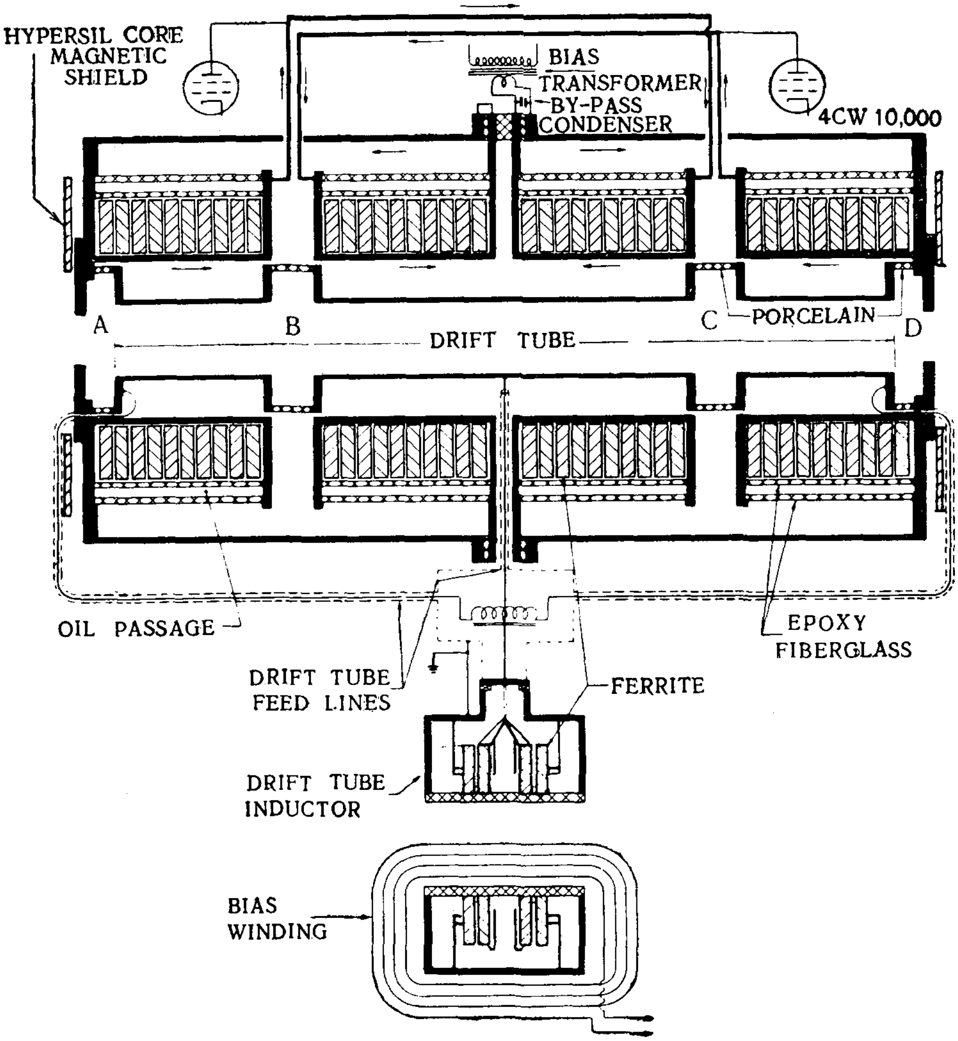

Fig. 7. Accelerator station.

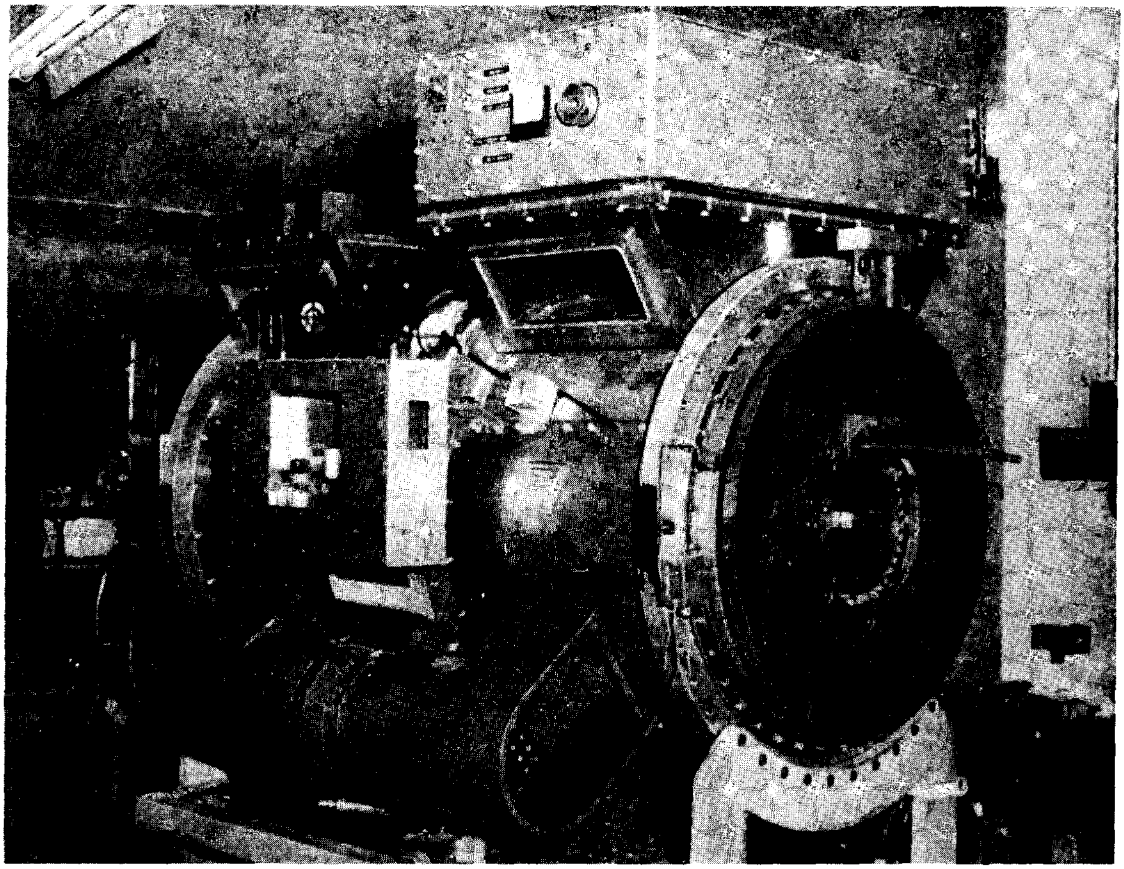

Fig. 8. Photograph of acceleration station.

into more detail than would be appropriate here. Our basic problem is to produce an accelerating voltage which varies in a precise way from zero to 120 kV, and back to zero at a frequency which varies by 12 : 1 from 2.43 MHz to 29.64 MHz in a time of 1/40 s. The initial capture frequency must be correct to at least $\pm$ 0.02% in order to avoid substantial beam loss.

We found it impracticable to resonate a high power ferrite loaded cavity over a frequency range of 12 : 1; so initial acceleration is provided by a ferrite loaded resonant drift tube system which operates from 2.4—6.5 MHz, and final acceleration occurs in a ferrite loaded double resonant cavity operating from 6.0 MHz to 30 MHz. In order to conserve space, the drift tube is placed within the cavity, each acceleration unit being driven by its own power amplifier. Fig. 7 shows one of four such acceleration stations. When operating in the drift tube mode, the three sections of drift tube are driven in parallel by coaxial cables and there is no power applied to the cavities; so a voltage appears across only gaps *A* and *D*. After cross over, when the cavity mode is powered and the drift tube is not, the main acceleration voltage appears across *A* and *C*. There is a brief period during the cross over when voltages appear across all four gaps.

Fig. 8 is a photograph of an acceleration station. Visible below the cavity is the transformer whose secondary delivers 14,000 A to bias the ferrite. Fig. 9 is a block diagram showing the complete radio-frequency system for one station. Though it is, of necessity, more complex than the usual synchrotron system, it does not differ very much in basic principles. Our problems arise from the large range of frequency, amplitude, rate of change of these quantities, and the high precision required. Also we must transfer acceleration from drift tube to

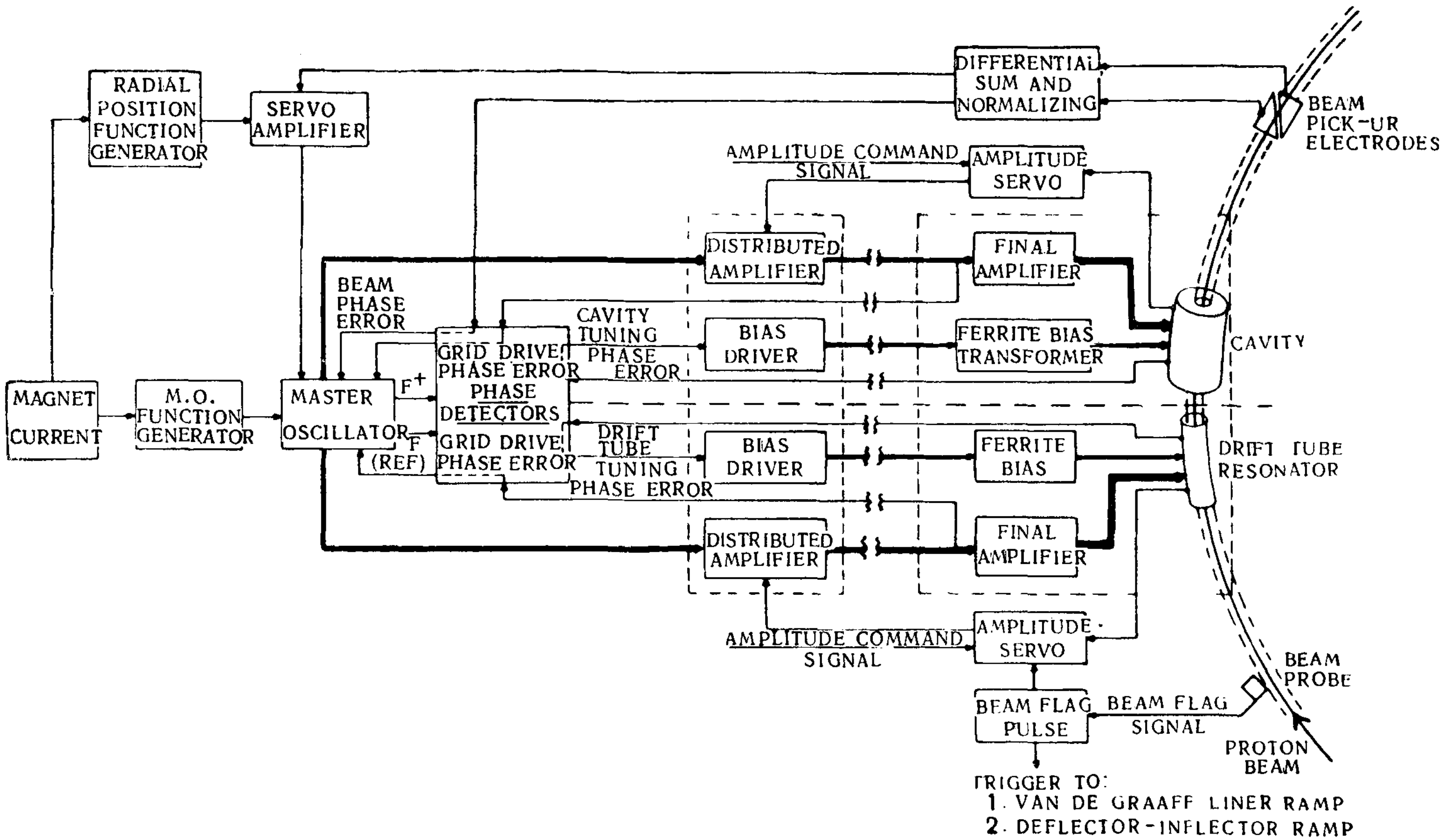

Fig. 9. Block diagram of radio-frequency system.

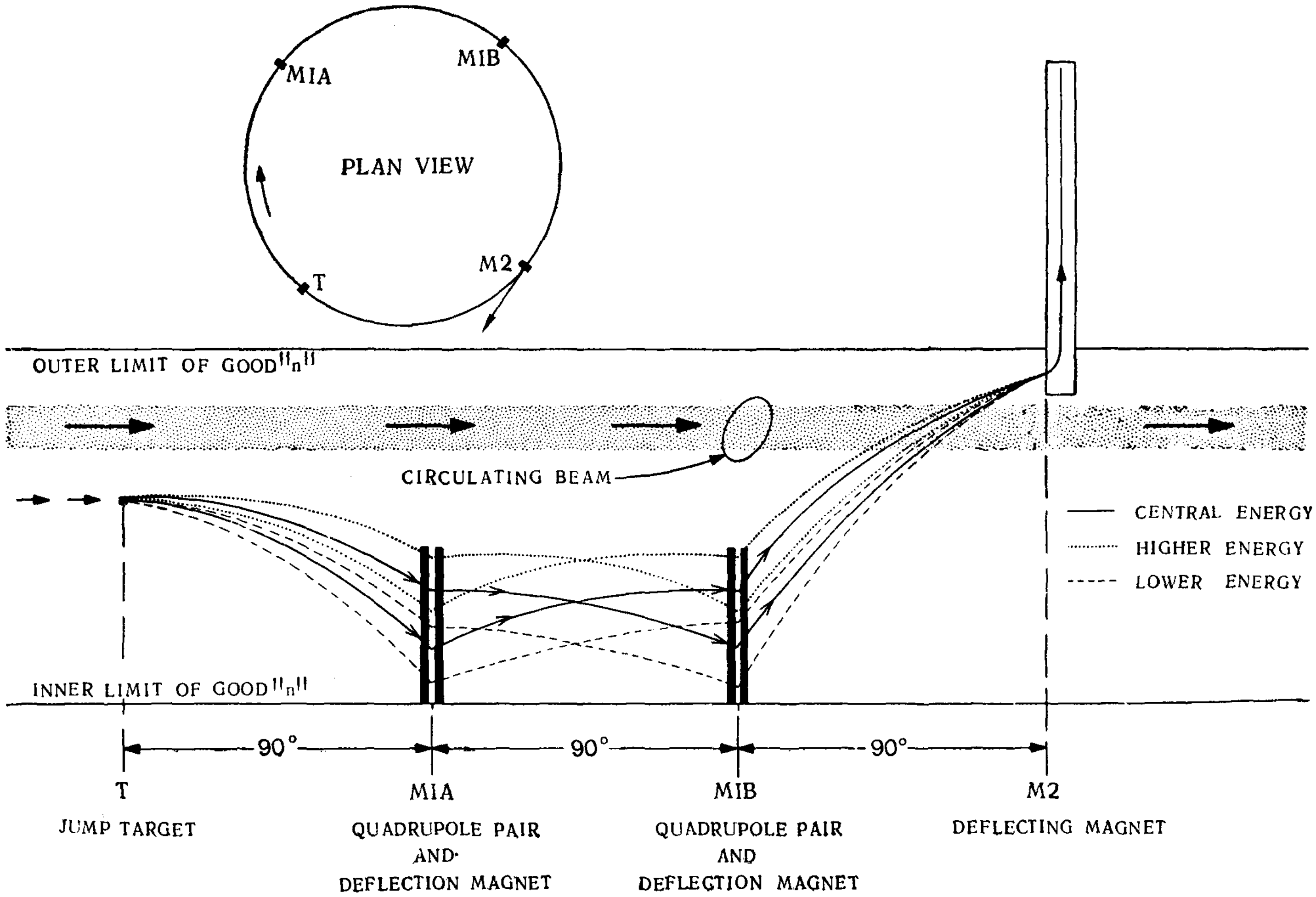

Fig. 10. Extraction system.

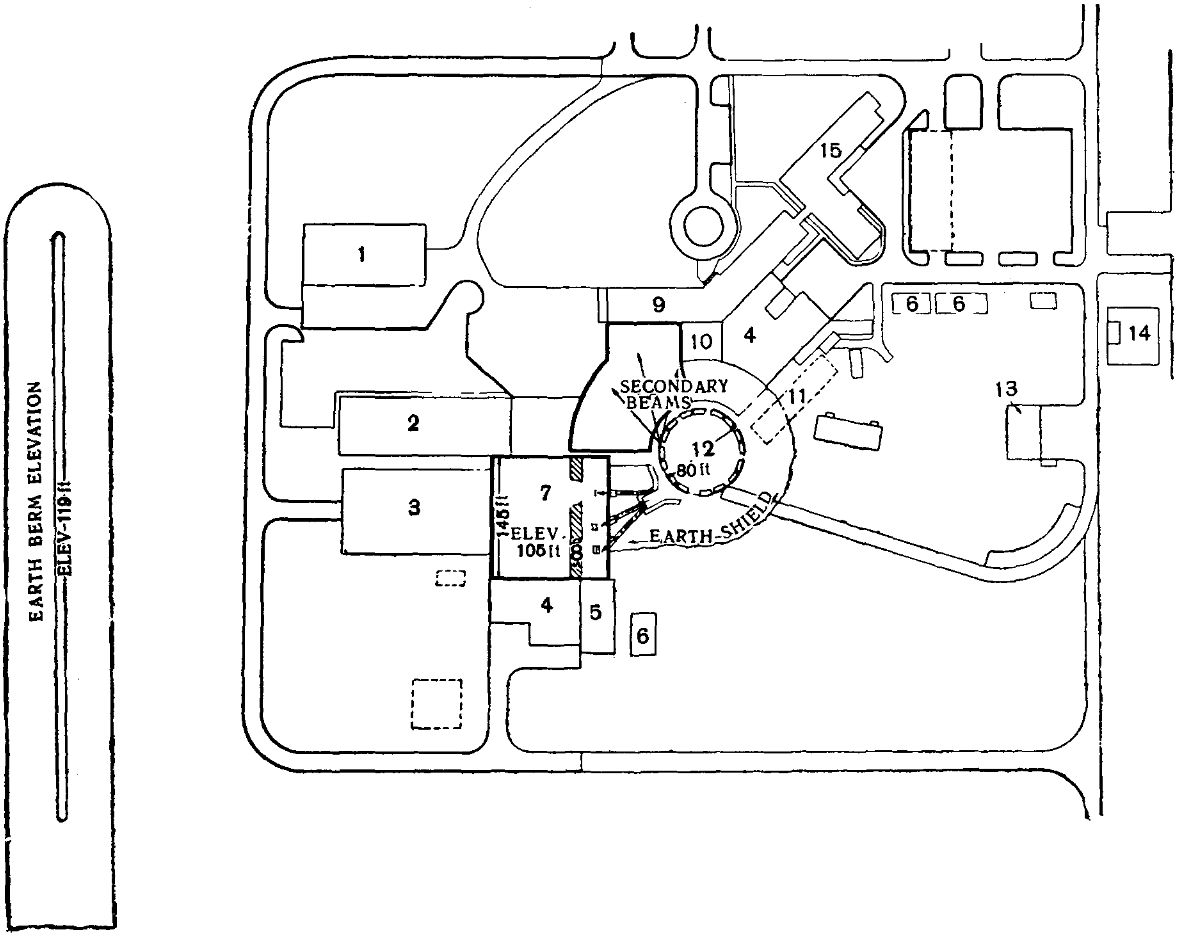

Fig. 11. Plan view of accelerator complex:
1 — storage and laboratory building; *2* — heavy support laboratory 8,000 ft^2; *3* — shielding storage pad; *4* — machinery room; *5* — substation No. 2; *6* — cooling tower, *7* — external proton beam target building; *8* — shield; *9* — research building; *10* — control room; *11* — future linac injector; *12* — synchrotron; *13* — liquid hydrogen test building; *14* — substation NoI; *15* —engineering and abministration building.

cavity quite carefully in order to avoid beam loss. This we have achieved with complete success, at least when the *RF* bucket size is small, and we believe this will be true for the largest bucket which will fit into our aperture.

8. BEAM EXTRACTION

Work is now going on to extract a long spill proton beam by an adaptation of Piccioni's system. Fig. 10 shows the system of magnets which will be used. The jump target, *T*, produces a 12 MeV energy drop and induces a radial betatron oscillation of 9 cm amplitude. The jump target also slightly scatters the beam and spreads it out in energy because of the statistical nature of the energy loss process. The RMS scattering angle is 1.3 mrad. In addition, residual betatron oscillations of protons hitting the target contribute to the energy spread of protons leaving the target, so that we finally end up with about a $\pm$ 0.1% energy spread. Because the synchrotron magnet is essentially a spectrometer with exceptionally large dispersion, the energy spread results in a spatial distribution as shown in Fig. 10. The solid curves correspond to the central energy, while the dotted curves are for the upper and lower energy limits. In order to «fold» these particles back together again we use a triple focussing arrangement which employs the synchrotron magnet as well as two quadrupole pairs with superposed uniform fields. Magnet MIA consists of a pair of current sheet quadrupoles (Panofsky type) each 2 feet (60 cm) long with gradients of approximately 2,500 Gs/inch (1000 Gs/cm) with a superposed uniform field of 600 Gs. Magnet M1B is identical to M1A, but with a superposed uniform field of 1000 Gs. The large quadrupole gradients are required because the magnets cannot be located at the optimum azimuthal position, but only where there are straight sections in the synchrotron magnet, and also because of the necessity of producing an **intermediate** space focus for each energy in order to produce a final energy focus. Magnet M2 must provide 13,000 Gs over 5 feet (1.5 m) to deflect the beam clear of the next semi-octant.

All three of these magnets, varying in weight from 150 lbs (68 kg) to 250 lbs (114 kg) must be moved in and out of the region of good «*n*» by a distance of 4 inches (10 cm) at a 19 cycle per second rate. Engineering problems are formidable, involving current densities of 120,000 A/sq. inch (19,000 A/cm^2), acceleration of 200 g or more, flexible high current leads and numerous other difficult mechanical problems. In addition, the currents in these magnets must be pulsed on and off in order to avoid interference with the synchrotron at low injection fields. According to calculations, the end result should be an extraction efficiency of 50%.

9. BUILDINGS AND FACILITIES

Fig. 11 shows the entire laboratory as it will be in 18 months. When completed, we will have 6,050 kVA for auxiliary magnets in the present, so-called, meson areas and 12,050 kVA in the External Beam Building. The total area for bombarding will be 37,000 sq. feet (3,441 m^2). Cooling water capacity for experimental purposes will be 18,600 kW in the summer and substantially higher in the winter.

ACKNOWLEDGEMENTS

Substantial contributions to the design and construction of the Accelerator have been made by the following: R. Brocker, P. Cheeseman, S. Frankel, T. Kitagaki, A. Mann, N. Oser, E. Ward, A. R. Trudel. Many others, too numerous to mention, have assisted with the design, construction, and many administrative details. Special acknowledgment should be made of the wholehearted support shown by the administration of Princeton University and the generous financial backing of the U. S. Atomic Energy Commission.

REFERENCES

1. White W. G., Shoemaker F. C., O' Neill G. K. CERN Symposium on High Energy Accelerators, v. 1, 1956, p. 525.
2. White W. G., Shoemaker F. C. In Proceedings of the International Conference on High Energy Accelerators and Instrumentation (CERN, 1959), p. 362.
3. Courant E. D. AGS Internal Report BNL-EDC-45.
4. Reardon P. J., Seidlitz L., and Shoemaker F. C. See this edition, p. 173.
5. Kirchgessner J.. O'Neill G. K., Riedel J. See this edition, p. 181.